

## MAPPING OF ANCIENT TEETH USING ABSORPTION OF ATR-FTIR SPECTROSCOPY AND LASER SCATTERING OF RAMAN SPECTROSCOPY

W. AL SEKHANEH\*

*Faculty of archaeology and Anthropology*

*Department of Conservation and Management of Cultural Resources*

*Yarmouk University, 21163 Irbid, Jordan*

This study was conducted on well-preserved archaeological teeth as an ancient biomaterial from the Roman period dated between the first and second centuries A.D in Jordan. Archaeological bone is an important witness as it records significant information about past societies and the situation of the teeth to use for conservation of archaeological bone. The morphological and structural changes in addition to the chemical composition of archaeological teeth material exhibit vital information about bone at different stages of the human development in biomaterials of paleo-diet, paleo-environment and paleopathology. In this study, vibrational spectroscopy, a combination of Attenuated total reflectance Fourier transform infrared(ATR-FTIR) spectroscopy and Fourier Transform Infrared Imaging (ATR-FTIRI) in addition to Raman as a laser spectroscopy and Raman imaging analyses were applied to 16 deciduous and permanent human teeth samples taken from a Roman archaeological site in Northern Jordan. The samples were examined for their mineral-to-matrix and carbonate to phosphate contents (at  $1412\text{ cm}^{-1}$  and at  $1030\text{ cm}^{-1}$  respectively)[1]. The study determines that the higher crystallinity and lower Carbonate to Phosphate C/P ratio in enamel than dentin are common features of dental tissues that have been confirmed.

(Received July 29, 2016; Accepted October 7, 2016)

*Keywords:* Ancient biomaterial, bone; collagen; Fourier transform infrared spectroscopy; Raman spectroscopy; imaging

### 1. Introduction

The bioarchaeology as new interdisciplinary field of research involves the common interests for chemists, archaeologists and anthropologists, the pathology and morphology of human biomaterials as bones, teeth and collagen that which recovered from archaeological sites preserve a good information for their evolutionary history[2], where the lock inside valuable record about the earlier life in Jordan region [3-5]. They retain information about the paleodiet[5-7], paleoenvironment[8], paleoclimate[9], and paleopathology[10], which can be extracted using a wide array of analytical methods [11] including spectroscopy [12-14].

Bone is a dense, semi rigid, porous, and calcified connective tissue composed chiefly of the inorganic matter calcium phosphate and calcium carbonate[15-17], as well as non-collagenous proteins and lipids as bio- materials [18-21]. The mineral phase in bone component consists of a poorly crystalline hydroxyapatite, where the replacement of phosphate in the matrix by carbonate increases the disordering of the lattice [22-24]. After death, the bones are influenced by the burial environment including soil composition, which alters the chemical composition of bones [25, 26]. Bones with high organic and low inorganic content are more susceptible to chemical decomposition or mechanical degradation than others[27, 28]. Bones and teeth have the properties of being hard and consistent containing a high mineral composition. Bones originate exclusively from mesodermal embryonic tissue, while teeth originate from both mesodermal and ectodermal

---

\*Corresponding author: sekhaneh@yu.edu.jo

tissue [29]. Teeth are essentially composed from several different layers: cementum, dentin and enamel [30, 31].

Enamel is the hardest and mineralized part of teeth, consisting of approximately 97% wt of crystallized hydroxyapatite (HA), the other 3% are bio-organic materials and water [32]. The dentin which makes up the tooth is less mineralized and less brittle than the enamel with 75% of hydroxyapatite (HA), 20% collagen and 5% water, but in the natural bone tissue, the (HA) consists of 69% calcium phosphate, 10% water, 20% collagen, and other organic material in small quantity [33-37]. All enamel, dentin, and the natural bone consist of (HA), which is a naturally occurring mineral form of calcium apatite with the formula  $\text{Ca}_5(\text{PO}_4)_3(\text{OH})$ . It crystallizes in the hexagonal crystal system [38, 39]. (HA) has many ionic substitutions in the lattice sites occupied by the anions and cations as carbonate, chloride, and magnesium interact with hydroxyapatite (HA) crystals in teeth, this interaction leads to de- and remineralization of enamel in vitro through the process of aging [40]. The hydroxyl ( $\text{OH}^-$ ) and phosphate ( $\text{PO}_4^{3-}$ ) in (HA) are substituted by carbonate ( $\text{CO}_3$ ) creating A-type and B-type carbonate respectively [23, 41-46]. Many researchers have studied the structures and properties of human dental carbonate [47-49] and have characterized structure-property in deciduous and permanent teeth [50, 51]. The mineral crystallinity, and crosslinking properties of dentin have been the subject of several studies reviewed elsewhere [52, 53].

The new development in photo-detection technique at the end of the 20<sup>th</sup> century has allowed the improvement of new solid state detectors for infrared spectra acquisition to be used simultaneously as a source of information in both spatial and spectral dimensions. This technique is referred to as "chemical imaging" [54-58]. Spectra are spatially located and it is possible to identify the chemical species inside the samples and also to map their distributions (Fig. 1). A chemical imaging experiment generates a three-way matrix called a data cube [59, 60]. Two dimensions,  $n$  and  $m$ , depict the spatial localizations of the chemical species and the third spectral axis allows their identification with a series of wave lengths [61]. Several thousand spectra are usually acquired using chemical imaging depending on the detector size. Therefore, the data are called multispectral or hyperspectral imaging (HSI) [62-64] and provide qualitative and analytical information in a spatially resolved manner [65-68]. Two dimensions depict the spatial distribution of the chemical compounds while the third one, the spectral dimension, allows the identification of the chemical compounds to determine the macroscopic distribution of these compounds.

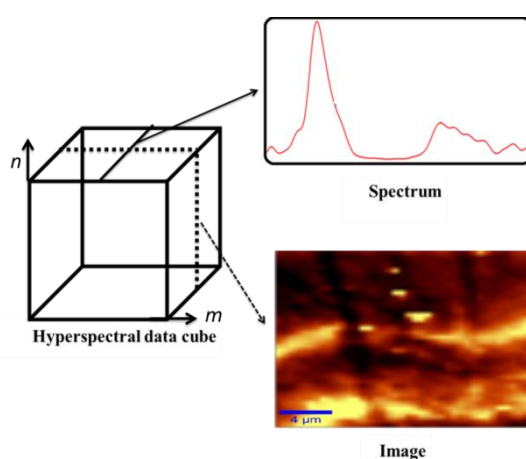


Fig. 1: Three dimensional data cube generated in the chemical imaging experiments.

To explore and assess the structure and function of the mineral and matrix of ancient bones in normal and diseased tissues, reviewed elsewhere, absorption infrared and laser scattering Raman imaging parameters can provide specific identification of solid state samples, organic—as well as inorganic compounds quantitatively and qualitatively [61, 68].

The Fourier Transform Infrared (ATR-FTIR)[69-71] micro-spectroscopy and Fourier Transform Infrared Imaging (ATR-FTIRI)[72, 73] constitute two sensitive techniques for obtaining molecular information to have a choice for degree detection of bone crystallinity as inorganic substance [74]. Both methods are non-destructive of the analyzed material contrary to more conventional methods, such as Mass Spectrometry (MS). (ATR-FTIR) micro-spectroscopy and (ATR-FTIRI) provide fast and reliable results about the molecular structure of bones and other hard tissues, such as, teeth.

Besides, the former can deliver spatially resolved data in micro-meters on the modification of bone structure and composition; the latter can identify a wide variety of materials and chemical bonds and produce distinctive molecular fingerprints. Accordingly, these methods are more frequently used than the conventional ones in investigating samples of a biological origin [75-80]. Most of the studies conducted on archaeological bone material using ATR-FTIR micro-spectroscopy focused on the preservation state of the bone mineral part [16, 17, 81, 82]. Only few studies have been concerned with a particularly interesting and non-trivial technique, which is the Raman spectroscopy in the analysis of biochemical changes in vivo cells and both soft and hard tissues upon progression of various changes[75, 83-87].

There are some studies on new teeth by nano-FTIR imaging of phosphate-based biominerals are demonstrated with a human tooth in which the bone-like phosphate nanocrystals are too small to be resolved, and the anisotropy or amorphous disorder in crystal of modern human teeth dentin will broad the band between 950-1150  $\text{cm}^{-1}$ [87-89]. An increasing in crystallinity of the archaeological bone and dentine in comparison to modern references by the crystallinity indexes and the splitting factors both are represented by broadening of ATR-FTIR and Raman bands of the apatite or carbonate in the samples [90, 91].

This study was conducted on well-preserved archaeological bone material from the Roman period dated between the first and second centuries A.D. at the archaeological site of Yasideh in Northern Jordan. Bones from this site provide material for the current study which aims to examine A & B-type carbonate as a function of age in human teeth [92, 93] by ATR-FTIR imaging and X-ray spectroscopy[94, 95].

## 2. Materials and Methods

### 2.1 Archaeological Site

Jordan is strategically located in the heart of the Middle East, the cradle of many civilizations-- and is known for its rich history and numerous archaeological sites especially in Northern Jordan. The archaeological site of Yasideh is located 9 km east of the city of Irbid and was occupied from the late Roman to the beginning of the Islamic Period. Excavation at the site started in 1988 and yielded information about the Roman and Byzantine periods in Northern Jordan to use for interpretation in the heritage of Jordan [96-98].

### 2.2 Sample Preparation

Sixteen teeth were collected from Yasideh archaeological site. Samples were collected if not affected by carious or sediment, they are well cleaned, and all were manually polished before testing with Alumina. The sample size for ancient dental elements used in this study is shown in Table 1.

*Table 1. The types of archaeological teeth*

Tooth types	Incisor	Canine	First Molar	Molar
Primary	1	1	1	x
Permanent	2	2	x	9

(Fig. 2) illustrates a photograph of a tooth cross section of one sample showing the component of the tooth, enamel, dentin and pulp. The position of the mapping is marked with 0.6 mm  $\times$  0.6 mm data squares in the left side of the image.

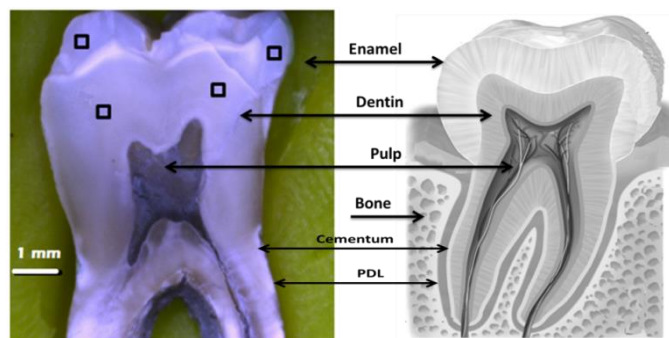


Fig. 2.A photograph of ancient tooth is illustrating enamel, dentin, pulp, cementum and periodontal ligament (PDL). Black squares indicate positions where the spectral map is scanned.

### 2.3 (ATR-FTIR) spectroscopy

Attenuated total reflectance Fourier transform infrared (ATR-FTIR) spectroscopy is a tool that has been used to probe chemical reactions/structure at the solid/liquid interfaces. Spectra were recorded using the imaging system combining a spectrometer (Varian 670-IR, USA) coupled with a variant microscope 64×64 focal plane array nitrogen (FPA) cooled detector was used to acquire the spectra in the interval of 900-4000 $\text{cm}^{-1}$  at a spectral resolution of 4  $\text{cm}^{-1}$ . Analysis were conducted in a reflection mode and equipped with attenuated total reflection (ATR) with a Germanium crystal (refractive index 4) and 64 scans were collected for each point; the array detector collects interferograms from its 4096 elements.

### 2.4 Raman spectroscopy

Two dimensional hyperspectral Raman images and spectra were collected by using a Raman micro-spectrometer (Kaiser Optical System, AnnArbor,MI, USA) emitted by a 785nm single mode external cavity diode laser of (Germany). All spectra were obtained using excitation power of 100mW with 100x/NA 0.9 objective (Nikon, Japan). Spectra were obtained over the spectral region of 300 to 1530  $\text{cm}^{-1}$  at a spectral resolution of 4 $\text{cm}^{-1}$  with a step size of 1  $\mu\text{m}$  with an accumulative time of 12 hours. Raman images were obtained using Confocal Raman microscopic system (alpha300 R; WITec Instruments, Germany) excited by a frequency doubled Nd:YAG laser at a wave length 532 nm focused onto the samples through a X20 Nikon objective with single spectrum acquisition time of 0.5 second, the data were processed using image plus software.

### 2.5 (ATR-FTIR) and Raman spectra analysis

As the regions of interest covered the pure dentin or enamel, ATR-FTIR and Raman spectra are analyzed by Origin Pro 8.5 ([www.originlab.com](http://www.originlab.com)) for Curve fitting processes for deconvolution of overlapping bands as 1030  $\text{cm}^{-1}$  in ATR-FTIR. The band numbers were resolved by calculating the second derivatives. The Gaussian band and manual linear baselines were applied.

### 2.6 Scanning Electron Microscope (SEM) and Backscattered Scanning Electron (BSE) microscopy

The investigations were carried out using an analytical scanning electron microscope (SEM) JSM-6300F (JEOL Ltd., Tokyo, Japan). The system is equipped with a cold field emission electron gun, which delivers high brightness and thus high resolution images. It operates at 30 kV with secondary electron image (SEI) resolution in the range of 1.5 nm. Correspondingly it operates at 5 kV approximately to achieve 5 resolutions. Besides the Everhart-Thornley detector type for secondary electrons is equipped with a semiconductor and a YAG scintillator type detector for back-scattered electrons (BSE). For analytical purposes an energy dispersive X-ray spectrometer with (Si(Li) detector type are cooled with liquid nitrogen; Oxford INCA) is present and enables element analysis on a nanoscale.

### 3. Results

#### 3.1 Raman and ATR-FTIR spectroscopy

The alterations between the dentine (top), and enamel (bottom) in (Fig 3) are determined with their shift and intensity of the bands such as the triplet at 2951  $\text{cm}^{-1}$ , 1658, 1454  $\text{cm}^{-1}$ , and 1265 are existed in dentin but not found in enamel, they distinguish more proteins component in dentin than enamel. Otherwise the inorganic hydroxyapatite component will be characterized by the major band at 962  $\text{cm}^{-1}$  and minor bands at 1072, 1049 and 589, 434  $\text{cm}^{-1}$ , all are present in both the dentin and enamel regions in (Fig. 2). Both spectra of dentin and enamel have been normalized to the 962  $\text{cm}^{-1}$   $\nu_1$  band phosphate  $\text{PO}_4^{-3}$  of hydroxyapatite. In (Fig 3) the relative heights of Raman spectra are roughly indicative of relative quantity of the components in the sample. The quantity of organic part in enamel is approached to zero as have seen in (Fig 3) while the existence of peaks in dentin between 1100 and 3000  $\text{cm}^{-1}$  indicates the presence of organic parts as collagen and amid. There is a mineral small peak is observed at 1072  $\text{cm}^{-1}$  related to carbonate.

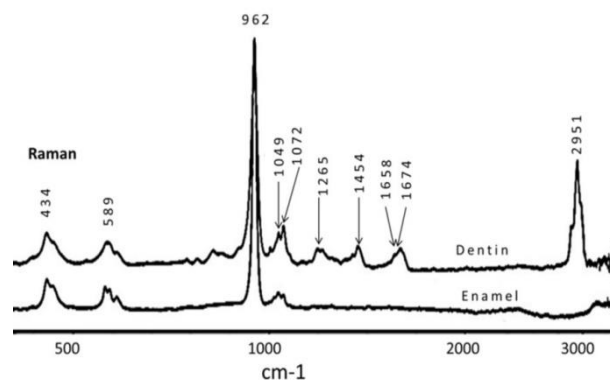


Fig 3. FT-Raman spectra of modern tooth, transverse section: dentine (top), enamel (bottom). In order to shift from normal spectra of vibrational spectroscopy we have to take more spectra to represent the mapping of the hard tissue.

(Fig. 4) and table 2 represent the typical ATR-FTIR (750-1800  $\text{cm}^{-1}$ ) and Raman spectra (800-1800  $\text{cm}^{-1}$ ) of human dentin and enamel. The ATR-FTIR difference spectrum between of dentin and enamel was calculated to better visualize the spatial of the organic and inorganic bands of the teeth. The ATR-FTIR spectra in region from 850-1200  $\text{cm}^{-1}$  is usually referred to mineralized bands  $\nu_1\nu_3$  of stretching  $\text{PO}_4^{-3}$  and the 1200-1800  $\text{cm}^{-1}$  region determines the protein region type I, Amide III CN stretching coupled with NH, collagen  $\text{CH}_2$ , Amide II/protein N-H band, C-N stretching, Amide I/ protein C=O or the other organic part of the teeth, which is collagen type I band [68, 99]. The significant shift of  $10 \pm 2 \text{ cm}^{-1}$  clearly performed on IR spectra of dentin and enamel related to the different contents of hydroxyapatite minerals from the enamel to the dentin or could be related to the mineralized tissue stress [99, 100]. The (ATR-FTIR) strong peak at 1006, 1019 and 1085  $\text{cm}^{-1}$  for the enamel and dentin respectively, assigned to be a component of the  $\nu_1$  and  $\nu_3$  phosphate envelope in poorly crystalline apatites attributed to  $\text{HPO}_4^{-2}$ . In the Raman spectra of the human hydroxyapatite both dentin and enamel, the bands associated with the mineral component appeared in the spectral range from 880 to 1100  $\text{cm}^{-1}$ , including  $\nu_1$  and  $\nu_3$  infrared vibration bands. Collagen components were observed in the spectral region of 1200 to 1700  $\text{cm}^{-1}$ . Moreover, the most intense peak on Raman spectra is the symmetric stretching vibration of  $\text{HPO}_4^{-2}$  at 962  $\text{cm}^{-1}$ ; in fact there is a weak peak that appears as a shoulder and its width is broad [100].

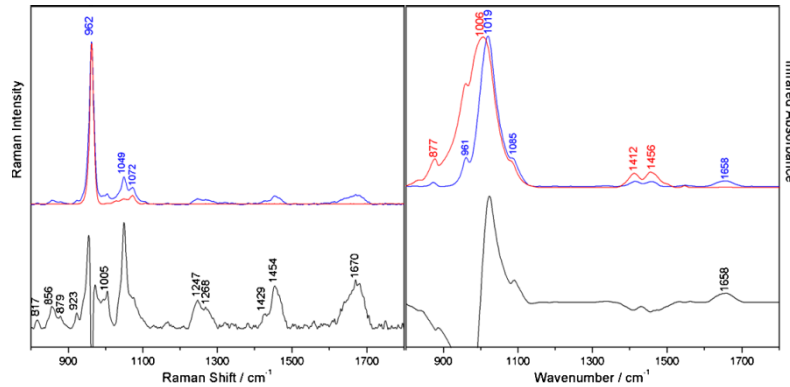


Fig. 4. Raman and FTIR spectra from 800 to 1800  $\text{cm}^{-1}$  of dentin (blue line) and enamel (red line). Difference spectra (dentin–enamel) visualize spectral contributions of organic matrix and collagen (black line).

Table 2: shows the peak representative assignments of both FTIR and FT-Raman spectra of enamel and dentin.

ATR-FTIR Peak $\text{cm}^{-1}$	Assignment	FT-Raman Peak	Assignment
877	$\nu_2$ of $\text{CO}_3^{-2}$	817, 856, 879, 923	Collagen
961	$\nu_1$ of $\text{PO}_4^{-3}$	962	$\nu_1$ of $\text{PO}_4^{-3}$
1006, 1019	$\text{HPO}_4^{2-}$	1005	Collagen
1085	$\nu_3$ of $\text{PO}_4^{-3}$	1049, 1072	$\nu_1$ of $\text{CO}_3^{-2}$
...	amide III	1247, 1268	amide III
1412, 1456	Type B $\text{CO}_3^{-2}$	1429, 1454	$\text{CH}_2$
1658	amide I	1670	amide I

The Mineral to matrix ratio is a measure of the mineral content of permanent (s1) and deciduous (s2) dentin. This, parameter is calculated as a ratio of the integrated area of the phosphate  $\nu_1$  and  $\nu_3$  of  $\text{PO}_4^{-3}$  ( $850\text{--}1200\text{cm}^{-1}$ ) to the amide I ( $1658\text{ cm}^{-1}$ ), the absorbance area under the band between ( $1610\text{--}1730\text{cm}^{-1}$ ) as shown in (Fig. 3). The area of this band is divided into the Amid I to yield a measurement of collagen integrity [101-103] therefore the ratio was shown as linearly related to the ash weight of a tissue. Therefore, it is indicative of the relative quantity of mineral in calcified tissue [104-106]. The mineral to matrix ratio was found to be the relationship between ATR-FTIR spectral parameters and the carbonate quantity percentages in the sample for imaging, respect to ATR-FTIR map of dentin and is different compared to Raman map (the average value was 6.4, with 4096 pixels of ATR-FTIR and the average value of mineral index of Raman dentin map was 3.8 with 4096 pixels).

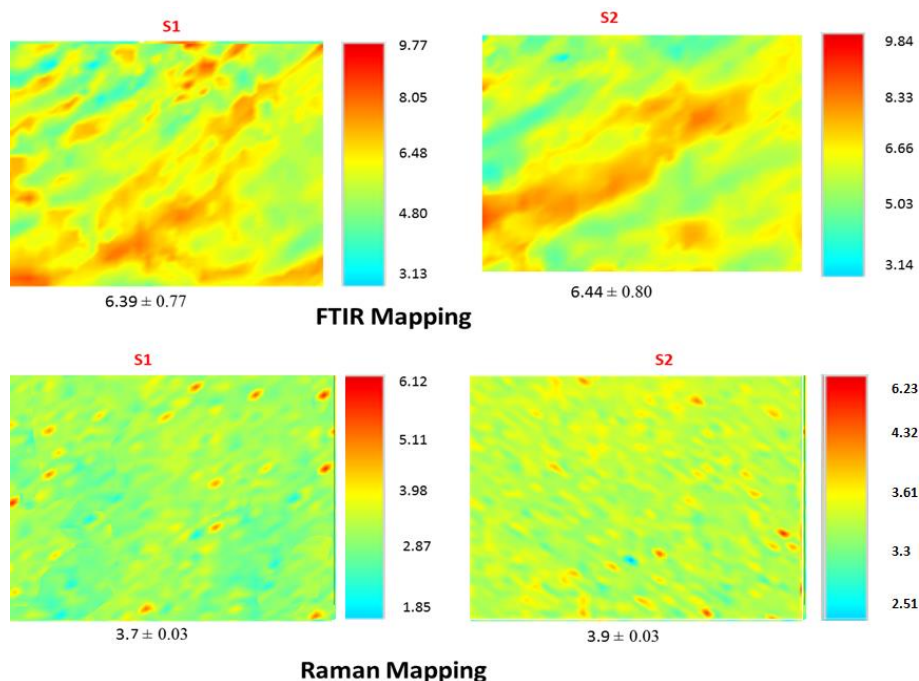


Fig. 5. ATR-FTIR, mineral to matrix ratio for permanent (S1) and (S2) deciduous dentin band of phosphate peak area of  $(850-1200) \text{ cm}^{-1}$  to the peak area of amide I peak  $(1610-1730) \text{ cm}^{-1}$  (top), Raman intensity ratio of mineral to matrix for permanent and deciduous dentin band of phosphate peak area of  $(850-1000) \text{ cm}^{-1}$  to the peak area of amide I peak  $(1610-1730) \text{ cm}^{-1}$  (bottom).

The mineral to matrix ratio of archaeological bone was obtained from the most intense mineral band of hydroxyapatite that is centered near  $1006 \text{ cm}^{-1}$  in ATR-FTIR spectra and near  $962 \text{ cm}^{-1}$  in Raman spectra and the most intense protein band of amide I band, centered near  $1658 \text{ cm}^{-1}$ . Each band area was determined by integration. The results of the mineral-to-matrix ratios the samples exhibited a large variations and were found to be inconclusive probably due to the effect of aging on the Amide group of the tooth matrix.

Fig. 6) illustrates the ATR-FTIR ratio of carbonate peak area to phosphate peak area was studied based on the intensity ratio of band B-type of carbonate which depicted at  $1412 \text{ cm}^{-1}$  to the peak of phosphate  $\text{PO}_4^{-3}$  at  $\nu_3$  mode at  $1030 \text{ cm}^{-1}$  (Fig. 7). The reason for the selected carbonate band at  $1412 \text{ cm}^{-1}$  is that the band does not overlap with the absorbance of other functional groups. The carbonate to phosphate (C/P) ratio was approximately comparable in both maps of Raman and ATR-FTIR and the average value of carbonate to phosphate C/P ratio is about 0.2. Furthermore, the Raman intensity ratio of mineral to matrix for permanent and deciduous dentin band of carbonate peak at  $(1072) \text{ cm}^{-1}$  to the peak area of phosphate at  $962 \text{ cm}^{-1}$ .

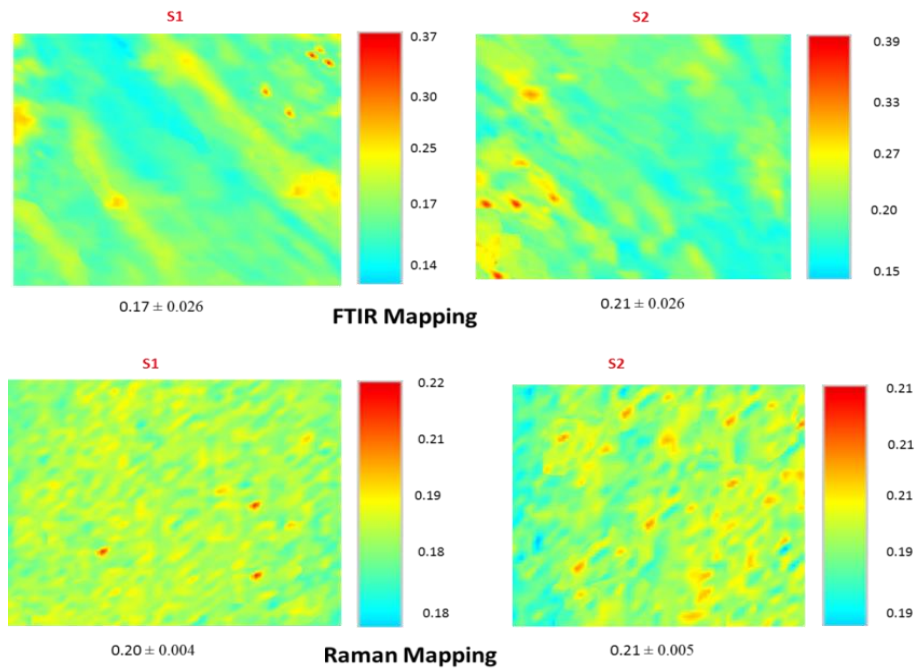


Fig. 6. ATR-FTIR, mineral to matrix ratio for permanent (S1) and (S2) deciduous dentin band of carbonate peak at  $1412 \text{ cm}^{-1}$  to the peak of phosphate at  $1030 \text{ cm}^{-1}$  (top), Raman intensity ratio of mineral to matrix for permanent and deciduous dentin band of carbonate peak at  $(1072) \text{ cm}^{-1}$  to the peak area of phosphate at  $962 \text{ cm}^{-1}$  (bottom).

The phosphate ATR-FTIR peak was fitted under the area from  $910$  to  $1160 \text{ cm}^{-1}$  with five components at  $961$ ,  $1006$ ,  $1019$ ,  $1030$ , and  $1085 \text{ cm}^{-1}$ . The band at  $961 \text{ cm}^{-1}$  is related to the  $\nu_1$  symmetric stretching vibration of phosphate,  $1019 \text{ cm}^{-1}$  is assigned to hydrogen phosphate ( $\text{HPO}_4^{2-}$ ) in crystalline apatite,  $1030 \text{ cm}^{-1}$  is linked to  $\nu_3$  vibration of  $\text{PO}_4^{3-}$ , and  $1085 \text{ cm}^{-1}$  is assumed to belong to stretching mode of the  $\text{PO}_2^{-1}$  group [107].

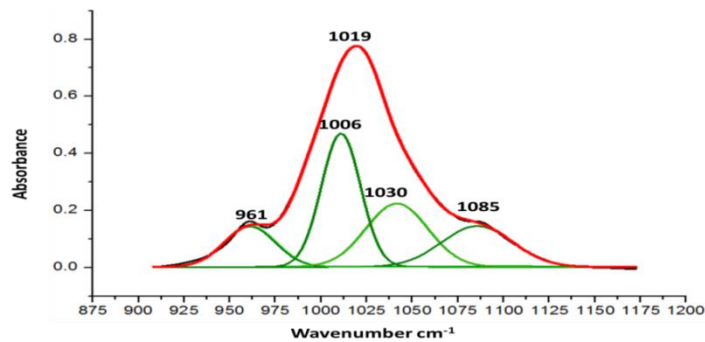


Fig. 7: Representative curve-fitting analysis of ATR-FTIR of phosphate band of permanent teeth spectra. The experimental spectrum (black) is overlapped with the renovated envelope (red) which is de-convoluted by the fitted curves (green).

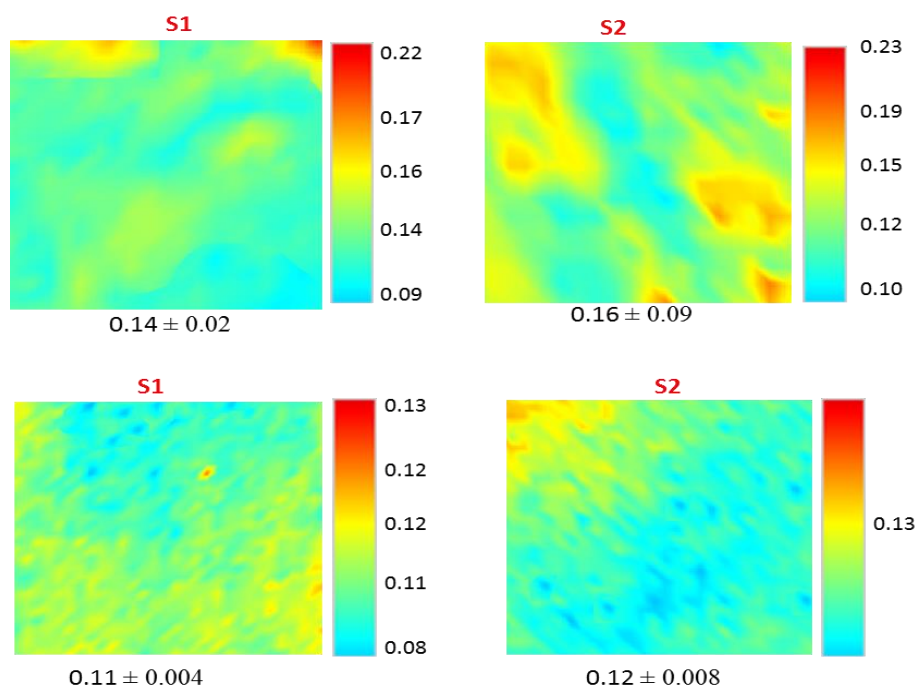


Fig. 8. ATR-FTIR, mineral to matrix ratio for permanent (S1) and (S2) deciduous enamel band of carbonate peak at  $1412\text{ cm}^{-1}$  to the peak of phosphate at  $1030\text{ cm}^{-1}$  (top), Raman intensity ratio of mineral to matrix for permanent and deciduous dentin band of carbonate peak at  $1072\text{ cm}^{-1}$  to the peak area of phosphate at  $962\text{ cm}^{-1}$  (bottom).

Table 3 summarizes the results of both Raman and ATR-FTIR spectroscopy of deciduous and permanent ancient teeth mapping from Jordan.

Tooth (sample)	ATR-FTIR	FT-Raman	Band $\text{cm}^{-1}$	Assignment
Permanent dentin (s1)	$6.44 \pm 0.80$	$3.9 \pm 0.030$	850-1200/1610-1730	Phosphate to Amid I
Deciduous dentin (s2)	$6.39 \pm 0.77$	$3.7 \pm 0.030$	850-1200/1610-1730	Phosphate to Amid I
Permanent dentin (s1)	$0.17 \pm 0.026$	$0.20 \pm 0.004$	1412/1030	Carbonate to Phosphate
Deciduous dentin (s2)	$0.21 \pm 0.026$	$0.21 \pm 0.005$	1412/1030	Carbonate to Phosphate
Permanent enamel (s1)	$0.14 \pm 0.020$	$0.11 \pm 0.004$	1412/1030	Carbonate to Phosphate
Deciduous enamel (s2)	$0.16 \pm 0.090$	$0.12 \pm 0.008$	1412/1030	Carbonate to Phosphate

Table 3 shows the average Phosphate to Amid I and carbonate to phosphate ratios in enamel and dentin obtained from ATR-FTIR and FT-Raman spectra. Figure 9 visualizes the spectral distribution images of minerals and organic parts in enamel and dentin in the region from  $300\text{--}1530\text{ cm}^{-1}$ .

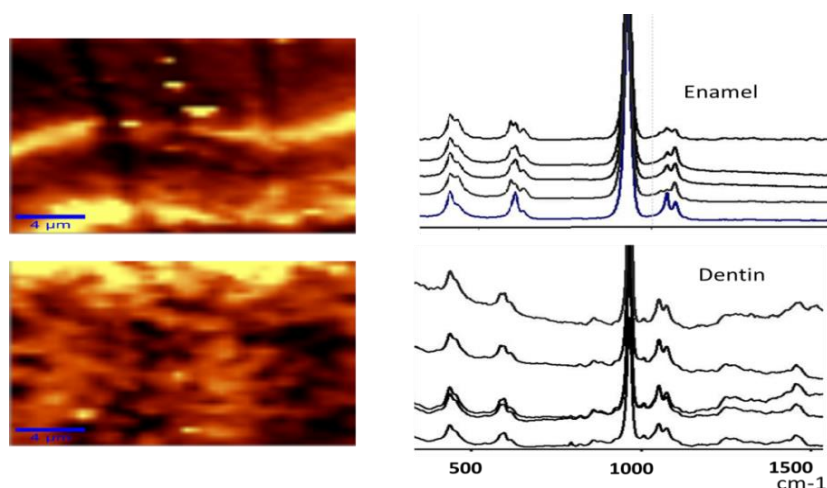


Fig. 9. Distribution images of minerals and organic parts in enamel and dentin in the region from  $300\text{--}1530\text{ cm}^{-1}$ .

The structural variation of enamel surface determined by both modes SEM and BSE micrographs, the microstructure is visible within the foci, similar to lamellar tunnels with about 10 micrometer length and 3 micrometer breadth.

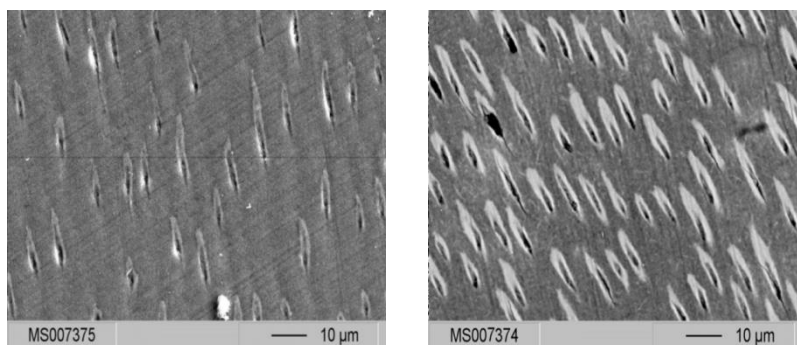


Fig. 10. Scanning electron micrograph shows the pores size in tooth enamel surface in the range of  $1\text{ }\mu\text{m}$  (left) Backscattered scanning electron (BSE) imaging and SEM image (right)

#### 4. Conclusions

This is a pioneering study in the field of archaeometry of ancient teeth ATR-FTIR mapping. There is no study concentrated and published on mapping of archaeological bone. For the first time, a combination of ATR-FTIR and Raman spectroscopy was applied to characterize ancient permanent and deciduous teeth. It concludes that the higher crystallinity and lower Carbonate to Phosphate C/P ratio in enamel than dentin are common features of dental tissues that have been confirmed by ATR-FTIR and Raman spectroscopy. The Phosphate to Amid I ratio, contribute the organic matrix including collagen; the ratio of permanent dentin is higher than the deciduous. Higher crystallinity and lower Carbonate to Phosphate C/P ratio were also observed in permanent teeth compared to deciduous teeth. These explanations conclude that the lower crystallinity and higher ratio of carbonate to phosphate in deciduous dentin contributes to their lower toughness and might be partly compensated by higher collagen cross-linking of the higher matrix content. The structure of ancient teeth is affected by degradation processes that harm the crystallinity of specimens by loss a quantity of organic part. The degradation of the organic matrix and the ratio of specific Raman bands, this was also observed for the carbonate to phosphate ratio, and the carbonate ions occupy two positions in the hydroxyapatite which is called a substitution of carbonate and phosphate in the hydroxide position of the enamel[108].

## Acknowledgments

The author is greatly indebted to all the team working in the Physical Chemistry at Jena University in Germany and DFG for financial supporting. Author is particularly grateful to Prof. Zeidoun Al-Muheisen, Dr. Susanne Ramadan for English editing and Prof. A. Al-Shorman, all for discussing this work and offering helpful suggestions.

## References

- [1] S. Gourion-Arsiquaud, et al., *Journal of Bone and Mineral Research*, **28**(1), 150 (2013).
- [2] S.H.Ambrose, J. Krigbaum, *Journal of Anthropological Archaeology*,. **22**(3), 193 (2003).
- [3] S.Weiner, O. Bar-Yosef, *Journal of Archaeological Science*, **17**(2), 187 (1990).
- [4] D.O.Henry, et al., *Bulletin of the American Schools of Oriental Research*, 1985, 45.
- [5] K. Al-Bashaireh, et al., *Radiocarbon*,. **52**(2), 645 (2010).
- [6] A.,Al-Shorman, *Journal of archaeological science*,. **31**(12), 1693 (2004)
- [7] A.Al-Shorman, L. El-Khouri, *Archaeological and Anthropological Sciences*, **3**(3), 263 (2011).
- [8] Y.Dauphin, C. Kowalski, and C. Denys, *Quaternary Research*, **42**(3): p. 340 (1994).
- [9] J.D. Bryant, B. Luz, P.N. Froelich, *Palaeogeography, Palaeoclimatology, Palaeoecology*, **107**(3-4), 303 (1994)
- [10] A.H.Goodman, , et al., *Indications of Stress from Bone and Teeth*. In: *Paleopathology at the Origins of Agriculture*. 1984.
- [11] H.J.,Park, et al., *Journal of Biomedical Materials Research Part A*, 2016.
- [12] M. C.,Stiner, et al., *Journal of Archaeological Science*, **22**(2), 223 (1995).
- [13] H. Edwards, et al., *Journal of Raman Spectroscopy*, **32**(1), 17 (2001).
- [14] T. Thompson, M. Gauthier, M. Islam, *Journal of Archaeological Science* **36**(3), 910 (2009)
- [15] V.C Mow, R. Huiskes, *Basic Orthopaedic Biomechanics & Mechano-biology*. 2005: Lippincott Williams & Wilkins.
- [16] R.,Shahack-Gross, et al., *Journal of Archaeological Science* **31**(9), 1259 (2004).
- [17] M. Lebon, et al., *Journal of Analytical Atomic Spectrometry* **26**(5), 922 (2011).
- [18] C.,Milner, *Functional Anatomy for Sport and Exercise: Quick Reference*. 2008: Taylor & Francis.
- [19] F.C.M.Driessens, R.K. Verbeeck, *Biominerals*. 1990: Taylor & Francis.
- [20] M.,Mucalo, *Hydroxyapatite (HAp) for Biomedical Applications*. 2015: Elsevier Science.
- [21] A., Al-Shorman, *Chemistry of Archaeological Bones*. First ed. 2013: Deanship of Scientific Research and Graduate Studies, Yarmouk University. 164.
- [22] R. Handschin, W. Stern, *Calcified tissue international*,. **51**(2), 111 (1992).
- [23] C.,Rey, et al., *Calcified tissue international*,. **45**(3), 157 (1989)
- [24] J. Harries, D. Hukins, S. Hasnain, *Calcified tissue international*,. **43**(4), 250 (1988)
- [25] M. R. Buzon, et al., *Handbook of archaeological methods*, **2**, 871 (2005)
- [26] A. Boddington, A.N. Garland, *Death, decay, and reconstruction: approaches to archaeology and forensic science*. 1987: Manchester University Press.
- [27] R.A. Nicholson, *Journal of Archaeological Science* **23**(4), 513 (1996)
- [28] G. Turner-Walker, *The chemical and microbial degradation of bones and teeth*. *Advances in human palaeopathology*, 2008: p. 3-29.
- [29] A.Boskey, R. Mendelsohn, *Journal of biomedical optics*,. **10**(3), 031102 (2005)
- [30] R. Gardner, *Development*,. **68**(1), 175 (1982).
- [31] J. Pispa, I. Thesleff, *Developmental biology*, **262**(2), 195 (2003).
- [32] D. Shi, *Introduction to Biomaterials*. 2006: Tsinghua University Press.
- [33] H. Xu, et al., *Journal of Dental Research*,. **77**(3), 472 (1998).
- [34] E. Beniash, et al., *Journal of structural biology* **166**(2): p. 133 (2009).
- [35] S. Park, et al., *Journal of Materials Science: Materials in Medicine* **19**(6), 2317 (2008).
- [36] C.W.,Gibson, et al., *Journal of Biological Chemistry*, 2001. **276**(34): p. 31871-31875.
- [37] J. D.Currey, *Bones: structure and mechanics*. 2002: Princeton university press.
- [38] J. C.Elliott, *Structure and chemistry of the apatites and other calcium orthophosphates*. 2013:

Elsevier.

- [39] L. Calderin, M. Stott, A. Rubio, *Physical Review B* **67**(13), 134106 (2003).
- [40] W. Van der Reijden, et al., *Caries research*,. **31**(3), 216 (1997).
- [41] J.M. Burnell, E.J. Teubner, A.G. Miller, *Calcified tissue international*, **31**(1), 13 (1980).
- [42] E. Boanini, M. Gazzano, A. Bigi, *Acta biomaterialia*,. **6**(6), 1882 (2010)
- [43] I.R.Gibson, W. Bonfield, *Journal of biomedical materials research*, **59**(4), 697 (2002)
- [44] J.,Barralet, et al., *Journal of Materials Science: Materials in Medicine*, **13**(6), 529 (2002).
- [45] E. Landi, et al., *Journal of the European Ceramic Society*, **26**(13), 2593 (2006).
- [46] A. Antonakos, E. Liarokapis, T. Leventouri, *Biomaterials*,. **28**(19), 3043 (2007).
- [47] R. Young, P. Mackie, *Materials Research Bulletin*,. **15**(1), 17 (1980).
- [48] R.Wilson, J. Elliott, S. Dowker, *American mineralogist*,. **84**(9), 1406 (1999)
- [49] A. Carden, M.D. Morris, *Journal of biomedical optics*,. **5**(3), 259 (2000).
- [50] M. Al-Jawad, et al., *Biomaterials* **28**(18), 2908 (2007)
- [51] I.,Low, N. Duraman, I.J. Davies. *Microstructure–Property Relationships in Human Adult and Baby Canine Teeth*. in *Key Engineering Materials*. 2006. Trans Tech Publ.
- [52] T. Leventouri, et al., *Crystal structure studies of human dental apatite as a function of age*. *International journal of biomaterials*, 2009. **2009**.
- [53] D. Magne, et al., *Journal of Bone and Mineral Research*, **16**(4), 750 (2001).
- [54] P. Mitchell, , et al., *Journal of inorganic biochemistry*,. **62**(3), 183 (1996).
- [55] P. Spencer, et al., *Journal of biomedical optics*,. **10**(3), 031104 (2005)
- [56] Y. Wang, X. Yao, R. Parthasarathy, *Journal of Biomedical Materials Research Part A*, **91**(1), 251 (2009).
- [57] Y.,Ling, et al., *Journal of Bone and Mineral Research*,. **20**(12), 2169 (2005)
- [58] P., Spencer, et al., *Dental Materials*,. **8**(1), 10 (1992)
- [59] J. Beltran, J. Guiteras, and R. Ferrer, *Analytical chemistry*, **70**(9), 1949 (1998)
- [60] K. C.Gordon, C.M. McGoverin, *International journal of pharmaceuticals*, **417**(1), 151 (2011)
- [61] C. Gendrin, Y. Roggo, C. Collet, *Journal of pharmaceutical and biomedical analysis*, **48**(3), 533 (2008).
- [62] A. Gowen, et al., *Trends in Food Science & Technology*,. **18**(12), 590 (2007).
- [63] G. Shaw, D. Manolakis, *IEEE Signal processing magazine*,. **19**(1), 12 (2002)
- [64] P.G. Lucey, K.A. Horton, T. Williams, *Applied optics*,. **47**(28), F107 ( 2008)
- [65] S. Sasic, Y. Ozaki, *Raman, Infrared, and Near-Infrared Chemical Imaging*. 2011: Wiley.
- [66] V.G.Gregoriou, M.S. Braiman, *Vibrational Spectroscopy of Biological and Polymeric Materials*. 2005: CRC Press.
- [67] M.D., Morris, *Microscopic and spectroscopic imaging of the chemical state*. 1993: CRC Press.
- [68] F.Severcan, P.I. Haris, and I. Press, *Vibrational Spectroscopy in Diagnosis and Screening*. 2012: IOS Press.
- [69] Y. Arai, D. Sparks, *Journal of Colloid and Interface Science*,. **241**(2), 317 (2001)
- [70] M.,Lebon, A. Zazzo, I. Reiche, *Palaeogeography, Palaeoclimatology, Palaeoecology*, **416**, 110 (2014).
- [71] G.H.,Yassen, et al., *Journal of endodontics*,. **39**(2), 269 (2013).
- [72] Y.,Xia, N. Ramakrishnan, A. Bidthanapally, *Osteoarthritis and cartilage* **15**(7), 780 (2007).
- [73] R.M. Coleman, et al., *Bone*, 2012. **51**(5): p. 920-928.
- [74] N. Pleshko, A. Boskey, and R. Mendelsohn, *Biophysical journal*,. **60**(4) 786 (1991).
- [75] K. Czamara, et al., *Analyst*,. **140**(7), 2164 (2015).
- [76] M. Pilarczyk, et al., *Vibrational Spectroscopy*,. **75**, 39 (2014).
- [77] P.P.Kundu, C. Narayana, *Journal of Medical & Allied Sciences*,. **2**(2), 41 (2012)
- [78] K. Majzner, et al., *Analyst*,. **138**(2), 603 (2013).
- [79] B. Singh, et al., *Application of vibrational microspectroscopy to biology and medicine*. *Current Science (Bangalore)*,. **102**(2), 232 (2012).
- [80] H.W.,Siesler, *Infrared and Raman Spectroscopic Imaging*. 2014: Wiley.
- [81] S. Weiner, P. Goldberg, O. Bar-Yosef, *Journal of Archaeological Science*, **20**(6), 613 (1993).
- [82] G. Boivin, et al., *Bone*, 2000. **27**(5): p. 687-694.
- [83] M. Pilarczyk, et al., *PloS one*,. **9**(8), e106065 (2014)

- [84] K. Kochan, et al., *Analyst*, **138**(14), 3885 (2013).
- [85] H. Nawaz, et al., *Analyst*, **135**(12), 3070 (2010).
- [86] J. Kneipp, et al., *Vibrational spectroscopy*, **32**(1), 67 (2003)
- [87] S. Amarie, et al., *Beilstein journal of nanotechnology*, **3**(1), 312 (2012)
- [88] S. Weiner, H.D. Wagner, *Annual Review of Materials Science*, **28**(1), 271 (1998).
- [89] N. Avery, et al., *Collagen: structure and mechanics*, 2008, Springer Science+ Business Media, LLC.
- [90] A. Olcott Marshall, C.P. Marshall, *Vibrational spectroscopy of fossils. Palaeontology* **58**(2), 201 (2015)
- [91] I. Reiche, C. Vignaud, M. Menu, *Archaeometry*, **44**(3), 447 (2002).
- [92] I. Davies, a comparative study of the microstructure-property relationship in human adult and baby teeth. in *Advances in Bioceramics and Biocomposites: A Collection of Papers Presented at the 29th International Conference on Advanced Ceramics and Composites*, Jan 23-28, 2005, Cocoa Beach, FL, Ceramic Engineering and Science Proceedings, Vol 26. 2009. John Wiley & Sons.
- [93] A. S. Clasen, I. Ruyter, *Advances in Dental Research*, **11**(4). 523 (1997).
- [94] Q. A. Acton, *Issues in Industrial, Applied, and Environmental Chemistry: 2011 Edition*. 2012: ScholarlyEditions.
- [95] E. DiMasi, L.B. Gower, *Biomaterialization Sourcebook: Characterization of Biominerals and Biomimetic Materials*. 2014: CRC Press.
- [96] Northern Jordan, A.B.S.I., *Tomb Reuse At Yasieleh: A Byzantine Site In Northern Jordan*. 2006.
- [97] A. Al-Shorman, *Mediterranean Archaeology and Archaeometry*. **6**(1) 43 (2006)
- [98] A. Al-Shorman, *Antiquity*, **78**(300), 306 (2004)
- [99] L. Wang, et al., *Mineralogical Magazine*, **71**(5), 509 (2007)
- [100] M., Anwar Alebrahim, et al., *Biomedical Spectroscopy and Imaging*, **3**(1), 15 (2014)
- [101] X., Bi, et al., *Analytical and bioanalytical chemistry*, **387**(5), 1601 (2007).
- [102] X., Wang, et al., *Calcified tissue international*, **71**(2), 186 (2002)
- [103] P.A., West, et al., *Journal of biomedical optics*, **10**(1), 014015 (2005).
- [104] D., Faibish, et al., *Bone*, **36**(1), 6 (2005).
- [105] D. Faibish, S.M. Ott, A.L. Boskey, *Clinical orthopaedics and related research* **443**, 28 (2006)
- [106] A.L., Boskey, *Elements*, **3**(6), 385 (2007)
- [107] S.Y. Lee, , et al., *Journal of veterinary science*, **10**(4), 299 (2009)
- [108] A.S. Clasen, I. Ruyter, *Adv Dent Res*, **11**(4), 523 (1997)